Hydrolytic Degradation and Biodegradation of Polylactic Acid Electrospun Fibers

Xiang Yun Debbie Soo,[1] Linran Jia,[2, 3] Qi Feng Lim,[1] Ming Hui Chua,[1, 5] Suxi Wang,[1] Hui Kim Hui,[1] See Jia Min Regine,[4] Yunjie Chen,[1] Jiuwei Li,[2, 3] Fengxia Wei,[1] Nikodem Tomczak,[1] Junhua Kong,[1] Xian Jun Loh,[1, 5, 6, *] Xunchang Fei,[2, 3, *] Qiang Zhu[1, 4, 5, *]

1. Institute of Materials Research and Engineering (IMRE), Agency for Science, Technology and Research (A*STAR), 2 Fusionopolis Way, Innovis, #08-03, Singapore 138634, Singapore.
2. School of Civil and Environmental Engineering, Nanyang Technological University, 50 Nanyang Avenue, Singapore 639798, Singapore
3. Residues and Resource Reclamation Centre, Nanyang Environment and Water Research Institute, 1 Cleantech Loop, Singapore 637141, Singapore
4. School of Chemistry, Chemical Engineering and Biotechnology, Nanyang Technological University, 21 Nanyang Link, Singapore 637371, Singapore
5. Institute of Sustainability for Chemicals, Energy and Environment (ISCE2), Agency for Science, Technology and Research (A*STAR), 1 Pesek Road, Jurong Island, Singapore, 627833, Republic of Singapore
6. Department of Material Science and Engineering, National University of Singapore, 9 Engineering Drive 1, #03-09 EA, Singapore 117575, Singapore

Corresponding authors: lohxj@imre.a-star.edu.sg; xcfei@ntu.edu.sg; zhuq@imre.a-star.edu.sg

Abstract

Increased use of bioplastics, such as polylactic acid (PLA), helps in reducing greenhouse gas emissions, decreases energy consumption and lowers pollution, but its degradation efficiency has much room for improvement. The degradation rate of electrospun PLA fibers of varying diameters ranging from 0.15 to 1.33 μm is measured during hydrolytic degradation under different pH from 5.5 to 10, and during aerobic biodegradation in seawater supplemented with activated sewage sludge. In hydrolytic conditions, varying PLA fiber diameter had significant influence over percentage weight loss ($W_{\%L}$), where faster degradation was achieved for PLA fibers with smaller diameter. $W_{\%L}$ was greatest for PLA-5 > PLA-12 > PLA-16 > PLA-20, with average $W_{\%L}$ at 30.7%, 27.8%, 17.2% and 14.3% respectively. While different pH environment does not have a significant influence on PLA degradation, with $W_{\%L}$ only slightly higher for basic environments. Similarly biodegradation displayed faster degradation for small diameter fibers with PLA-5 attaining the highest degree of biodegradation at 22.8% after 90 days. Hydrolytic degradation resulted in no significant structural change, while biodegradation resulted in significant hydroxyl end capping products on the PLA surface. Scanning electron microscopy (SEM) imaging of degraded PLA fibers showed a deteriorated morphology of PLA-5 and PLA-12 fibers with increased adhesion structures and irregularly shaped fibers, while a largely unmodified morphology for PLA-16 and PLA-20.

Keywords: Polylactic acid, biodegradation, hydrolytic degradation, electrospun fibers, sustainability

1. Introduction

Conventional plastics pose significant environmental damage due to their slow degradation, leading to their persistence in the environment and widespread pollution. This is especially evident during the Covid-19 pandemic, where PE based facemasks were irresponsibly disposed and led to severe pollution of land and sea.(Benson et al., 2021; Dharmaraj et al., 2021) To address this pollution issue, there is a growing shift toward biodegradable plastics, (Atiwesh et al., 2021; Muiruri et al., 2023; Pang et al., 2023; Png et al., 2023; Sarasa et al., 2009; Wang et al., 2022b) notably PLA.(Yusoff et al., 2021) PLA, derived from renewable sources like corn starch or sugarcane, is biodegradable and compostable, offering a sustainable alternative to traditional plastics.(Madhavan Nampoothiri et al., 2010) It is widely used in applications such as biomedical implants, drug delivery systems, food packaging, clothing and textiles, agricultural films, thermal energy storage or compostable bags etc.(Brodin et al., 2017; Cui et al., 2020; Dong et al., 2023; El-malek et al., 2020; Fan et al., 2017; Lagaron and Lopez-Rubio, 2011; Lee et al., 2022; Liang et al., 2022; Loh, 2013; Nguyen et al., 2011; Soo et al., 2023; Soo et al., 2022a; Tang et al., 2022; Wang et al., 2023; Wang et al., 2022c) The life cycle assessment (LCA) of PLA has shown its potential to reduce greenhouse gas emissions by as much as 50-70%,(Álvarez-Chávez et al., 2012; Muiruri et al., 2022) signaling a good solution to mediate the pollution problem.

Currently there are different strategy to reduce or degrade substances via chemical catalysis or relevant treatment.(Cui et al., 2017; Guo et al., 2023; Zhao et al., 2023; Zheng et al., 2020) PLA is degradable via different methods such as hydrolytic, thermo, bio etc., and degradation is often initiated at the polar carbonyl groups.(Amorin et al., 2014) The PLA crystallinity, morphology, molecular weight, as well as degradation conditions like pH and temperature can affect the rate of degradation.(Araque-Monrós et al., 2013) For hydrolytic degradation, many studies have been

carried out at different pH to compare the degradation rates. Different range of sizes and microstructures of PLA were found to degrade fastest in alkaline conditions compared to acidic and neutral conditions, and a decrease in mechanical strength and increase in crystallinity often accompanies it.(Vaid et al., 2021; Xu et al., 2011) Araque-Monrós et al.(Araque-Monrós et al., 2013) degraded hollow braided PLA at pH 3, 7.4 and 12 at 37 ºC over 12 months, of which fiber diameter was about 18.6 μm. There was a 21% weight loss and more significant morphological changes for PLA degraded in the alkaline media but no substantial change for the rest. Nevertheless, average molecular weight and mechanical properties decreased for all samples. While Vaid et al.(Vaid et al., 2021) degraded PLA fibers of about 10-15 μm in diameter under a pH environment of 2, 3, 7.4 and 10 over 25 days. Likewise, hydrolytic degradation occurred the fastest in basic environment (pH 10) with mass loss of 0.6%, which was about four times greater than PLA in the other pH solutions. This was accompanied by a drop in mechanical properties where PLA exposed to pH 10 reduced by 40% and the others by 25%. Similarly, Xu et al.(Xu et al., 2011) degraded PLA brushes of 10nm thick in pH 8, 7.4, 7, 6 and 3. The more basic solutions, pH 8 and 7.4, were more efficient in removing PLA brushes from its substrate in 25 h and 100 h respectively. The neutral solution took a much longer time of 450 h, while the remaining two acidic conditions displayed no significant change.

Several studies have also been investigated for the performance of PLA during the biodegradation process in sewage sludge. Research by Richert et al.(Richert and Dąbrowska, 2021) demonstrated the biodegradation efficiency of PLA under different environments. The study proved that the microbial consortia present in activated sludge and compost leads to a better hydrolysis of chemical bonds and decomposition of PLA than those from sea or river water. The potential of

sewage sludge as medium for the biodegradation of PLA is further supported by Campanaro et al.(Campanaro et al., 2023), whose work discovered degradation rates of aged and non-aged PLA in the presence of sewage sludge. This research indicated the importance of prior photo-degradation of plastics before entering the wastewater treatment system to promote the activity of specific microorganisms efficiently degrading PLA within sewage sludge.

When taking a closer look at degradation rates of PLA or PLA modified polymers as a function of particle size, Grizzi et al.(Grizzi et al., 1995) showed a clear distinction in degradation rates for polylactide-co-glycolide (PLGA) thickness at different order of magnitudes under a condition of pH 7.4 at 37 ^{o}C. Degradation occurred faster at greater thickness; plates > milli or micro spheres > films. This was due to the auto-catalytic effect where degraded materials with carboxylic chain ends were trapped within the matrix of thicker PLAGA, creating an acidic environment to auto-catalyze the degradation process. Thinner PLAGA allows for faster diffusion of these degraded materials out of the matrix and undergoes smaller extent of degradation. Dunne et al.(Dunne et al., 2000) also demonstrated a clear dependence of particle size for hydrolytic degradation using PLAGA, but on a similar order of magnitude. PLGA particles of three different sizes, < 1 μm, < 20 μm, and < 50 μm were incubate in PBS pH 7.4 at 37 ^{o}C, and the larger PLGA particles were found to degrade faster. The auto-catalytic effect eventually caused PLGA to lose their structure and increase in porosity for degraded materials to diffuse out. However, these comparisons are of sizes with significant difference, and conducted at physiological conditions (pH 7.4). Hence it will be interesting to study different PLA fiber thickness at a smaller scale (0.15 to 1.33 μm) to see how the degradation is affected.

During the recent Covid-19 pandemic, there was a rise in production of biodegradable PLA face masks in a bid to reduce environmental pollution from disposable polyethylene based face mask.(Choi et al., 2021; Garcia et al., 2021; Morganti and Morganti, 2020; Morganti et al., 2020) PLA based masks(He et al., 2020; Patil et al., 2021; Wang et al., 2022a) attained particle filtration performance ≥ 95 wt%, comparable to that of N95/KN95 masks. In our previous work,(Soo et al., 2022b) we monitored the degradation of a whole piece of PLA mask in pH 2, 7 and 13 at room temperature for 4 weeks. Similar to other works, degradation was greatest in the alkaline environment, but minimal effects in acidic and neutral environment. Through SEM imaging, we found greater hydrolytic and biodegradation features for the thinner middle meltblown layer compared to the thicker outer spunbond layers, however there was no quantifiable measurements, and more so on how different pH affects hydrolytic degradation of PLA fibers with different diameters. Most of the available literature monitors degradation as a function of particle size in PBS as their applications are for the human body. To fully understand the effect of fiber thickness on the degradation rate, PLA fibers of different diameters can be fabricated via electrospinning (Lim et al., 2023; Zhang et al., 2023) and subjected to degradation tests. In this article we describe the fabrication of fibrous mats made of electrospun PLA of different fiber diameters from 0.15 μm to 1.33 μm. The mats were then subjected to hydrolytic and microbial degradation. To mimic physiological and ambient conditions the fibers were soaked in four aqueous solutions with pH values ranging from pH 5.5 to 10, and the temperature was maintained at 37 ºC. It was noted that the Tg of PLA is 60 ºC, and degradation when carried out above its Tg would be much more efficient.(Mitchell and Hirt, 2015) However, the degradation temperature was chosen based on the intended application or eventual environment it might end up in after disposal. This is so that the lab scale tests can mimic as closely to the environmental conditions as possible. Weight loss of the

PLA fibers was used to monitor the degradation. FTIR and SEM analysis were performed to study the chemical and physical degradation, respectively. Biodegradation tests were conducted according to international standard methods OECD 301B and 306(OECD, 1992a; OECD, 1992b) with slight modifications, where carbon dioxide production, total organic carbon content and weight loss were monitored.

2. Materials and Methods

2.1 Materials

1,1,1,3,3,3-hexafluoro-2-propanol (HFP), hydrochloric acid, sodium hydroxide and phosphate buffered saline was purchased from Sigma-Aldrich. PLA was purchased from Nature Works (3051D, 96.5% of L-lactide, Mw = 160,000, PDI = 1.7). All chemicals were used without further purification.

2.2 PLA fibers fabrication

PLA/HFP solutions with different PLA concentration (5 w/v%, 12 w/v%, 16 w/v% and 20 w/v%) were prepared.(Lim et al., 2023) The PLA/HFP solution was loaded into a syringe and connected to a needle (25G for inner diameter). Using a rotating drum with a width of 120 mm as the collector, electrospinning of PLA/HFP was carried out under the following parameters: feeding rate of 1.2 mL/h, environmental humidity of 50 ~ 70 RH%, voltage of 15 kV, needle tip-to-drum top distance of 13 cm, and drum rotation speed of 50 rpm. The needle is set in a to-and-forth motion with speed of 30 mm/s and distance of 140 mm perpendicular to the drum rotation axis.

2.3 Hydrolytic Degradation

Aqueous solutions with pH 5.5 were prepared by diluting 37% hydrochloric acid with deionized water. pH 8 and 10 solutions were prepared by dissolving sodium hydroxide pellets in appropriate volume of deionized water. pH 7.4 solution was prepared using phosphate buffered saline tablet. PLA fibers were cut into an appropriate size, and the weight W_i was recorded. The fibers were then placed in the respective pH solutions and kept at 37 ºC in an oven to soak for 1, 2, 3, 4, and 8 weeks. After soaking for the respective durations, the fibers were collected, rinsed with deionized water, and dried at 37 ºC for 2 days. After drying, the fiber weight W_f was measured. The percentage weight loss $W_{\%L}$ was then calculated by:

$$W_{\%L} = \frac{W_i - W_f}{W_i} x\ 100\% \qquad (1)$$

2.4 Aerobic biodegradation tests

The biodegradation tests of PLA fibers were conducted according to international standard methods OECD 301B and 306 (OECD, 1992a; OECD, 1992b) with slight modifications. Briefly, the biodegradability of PLA fibers was determined by the analysis of carbon dioxide (CO_2) evolution from accelerated aerobic biodegradation process in seawater supplemented with activated sewage sludge. The sludge was obtained from a wastewater treatment plant in Singapore one week prior to the biodegradation tests. The mixture of seawater and sludge was pre-filtered to remove coarse suspended particles and pre-aerated at room temperature of 25 ºC for one day before inoculation. The PLA fibers and reference ashless cellulose filters were cut into 1 cm × 5 cm pieces in advance. The total organic carbon (TOC) contents of test materials were measured by a TOC analyzer (Shimadzu, Japan).

For each test, 100 mg sample with about 50 mg TOC was immersed in the inoculation solution in a conical flask with a total suspended solids (TSS) content of 300 mg/L to achieve a final liquid volume of 200 ml. CO_2-free air was bubbled into the solutions at a rate of 30 ml/min to maintain aerobic condition, while each flask was stirred using a magnetic stirrer. All the samples were tested in duplicates for 90 days under 24 ± 2 °C. The generated CO_2 was channeled to another flask and absorbed by KOH solution, which was analyzed by an auto-titrator and replenished every week (Mettler Toledo, USA). The biodegradation degree of each sample was calculated by dividing the amount of measured CO_2 generation by the amount of theoretical CO_2 generation ($ThCO_2$) calculated from the TOC value (a detailed calculation formula can be found in the Supporting Information), which was expressed in percentage.(ISO, 2020) The final dry weight of each sample was measured by the end of the test and the weight loss was calculated. It is noted that the weight loss value indicates the amount of sample that was altered through biodegradation, solubilization and fragmentation, while the biodegradation value suggests the amount of sample that was converted into carbon dioxide due to bio-mineralization.

2.5 Characterization

Scanning electron microscope (SEM), Heliso 600 DualBeam, Thermofisher/FEI, with e-beam voltage of 2 keV and image resolution of 1 nm was used to examine the morphology of the PLA fibers at various pH conditions after each degradation interval. The diameter of the fibers was measured using SEM images and a software ImageJ. Fourier-transform infrared spectroscopy for quantitative and qualitative analysis of PLA fibers was performed using Spectrum 2000, PerkinElmer, USA in a range of 4000 to 600 cm^{-1}. A total of 16 scans were executed at a resolution of 4 cm^{-1}.

2.6 Analysis of variance (ANOVA)

Two-way ANOVA with replication was carried out to measure the groups difference and interaction for PLA diameter (PLA-5, PLA-12, PLA-16, PLA-20) and pH of soaking solution (10, 8, 7.4 and 5.5) at each time point (Week 1, 2, 3, 4, 8). $P < 0.05$ and $F > F_{crit}$ was considered to indicate statistical significance. The analysis was conducted using Microsoft Excel.

3. Results and Discussion

3.1 Preparation and Characterization of Electrospun Fibers

PLA degradation has been widely studied in the bulk,(Luo et al., 2012; Ozdemir et al., 2016) film(Iñiguez-Franco et al., 2017; Kalendova et al., 2019; Limsukon et al., 2019) and fiber(Santoro et al., 2016; Surrao et al., 2012) forms, but most of the studies were focused on the effects of additives or environmental conditions on the degradation rate, and the effect of fiber size was not considered. Electrospinning allows for the fabrication of PLA fibers with different diameters by controlling PLA/HFP concentration, i.e., higher concentration leads to larger diameter. PLA was electrospun into fibrous mats with four different fiber diameters, forming a free-standing membrane with interconnected pores and tortuous channels. The PLA fibers are solid and non-porous with relatively smooth surface and some minor cracks that most likely caused by the electrical stretching force during electrospinning (Figure S1a_1 & a_2, b_1 & b_2, c_1 & c_2, d_1 & d_2). The diameter distributions of the fibers, as presented in Figure S1a_3, b_3, c_3 and d_3, show mean diameter of 0.15, 0.62, 0.84 and 1.33 μm, corresponding to a PLA/HFP concentration of 5, 12, 16 and 20 w/v% (PLA-5, 12, 16, 20), respectively. It is noted that PLA-5 fibers were non-uniform in diameter

and had many beads, suggesting that low PLA/HFP concentration cannot ensure a smooth electrospinning due to insufficient viscosity and PLA feeding.

FTIR spectrum of the PLA fibers correlates well with the PLA chemical structure, where the characteristic bands are observed for C=O stretching around 1749 cm^{-1}, CH_3 asymmetric bending around 1452 cm^{-1}, and C–O stretching around 1182 and 1084 cm^{-1} (Figure S2a).(Oliveira et al., 2016; Soo et al., 2023) FTIR confirmed that no chemical reaction took place during the electrospinning process and that pure PLA fibers were used in the subsequent analysis.

3.2 Hydrolytic Degradation

Hydrolytic degradation of the electrospun PLA fibers was studied in a pH environment of 5.5, 7.4, 8 and 10 over a period of 8 weeks. The samples were maintained at 37 ^{o}C to mimic the body and tropical temperature conditions. Fiber weight loss was recorded at regular time points over the course of the degradation period of 8 weeks, and the percentage weight loss ($W_{\%L}$) and was calculated (Table S1) and a two-way ANOVA with replication was performed for results at each time point (Table S2). The ANOVA indicated a significant relationship between PLA diameter and $W_{\%L}$ ($P < 0.05$, $F > F_{crit}$), but no significant relationship between environmental pH and $W_{\%L}$ nor any significant interaction between PLA diameter and pH to influence $W_{\%L}$ ($P > 0.05$, $F < F_{crit}$) at all time points. Hence, difference in PLA diameters have a significant influence over the degradation rate of PLA.

Weight loss was detected for all PLA fibers of different diameters regardless of the pH environment. The PLA fibers with a smaller diameter had a higher degradation (Figure 1a-d), where $W_{\%L}$ was

highest for PLA-5 > PLA-12 > PLA-16 > PLA-20. The average $W_{\%L}$ for each fiber diameter was 30.7%, 27.8%, 17.2% and 14.3% respectively. This trend suggests that surface erosion took place to a greater extent than bulk erosion, which is supported by the SEM imaging (**Error! Reference source not found.Figure 1**) where smooth, regular shaped fibers becomes rough and deformed, but with little or no pores. Bulk degradation occurs when the degradation media diffuses faster into PLA than the degradation products with acidic caping end groups defuse out, leading to auto-catalytic effect from the trapped products. Larger particles lead to slower outward diffusion of degraded products, hence faster degradation rate by auto-catalytic effect and greater porosity in the structure.(Dunne et al., 2000; Grizzi et al., 1995) This is opposite from the trend observed for the PLA fibers. Electrospun fibers tend to have a higher degree of crystallinity due to stretching of the fibers during electrospinning, which makes it harder for the hydrolysis media to penetrate the fibers. (Vaid et al., 2021)As such surface erosion dominates, and smaller diameter PLA fibers would be more susceptible to hydrolysis as there is a larger surface area exposed to the hydrolytic media for degradation. Thus, the smaller diameter fibers would achieve a faster degradation rate with higher $W_{\%L}$ as detected in this study.

Different pH environment does not have a significant influence on the PLA degradation, where the PLA fibers of the same diameter seem to attain almost similar $W_{\%L}$ for all conditions (Figure 1e-h). Nevertheless, PLA fibers soaked in higher pH solutions does overall perform slightly better, (Soo et al., 2022b; Vaid et al., 2021; Xu et al., 2011) which could be due to faster hydrolysis by direct attack of the carbonyl carbon by excess OH^-. While acid catalyzed hydrolysis tends to be slower as it involves a larger and more sterically hindered water molecule (H_2O) as the nucleophile in addition to the need for carbonyl activation.(Vaid et al., 2021)

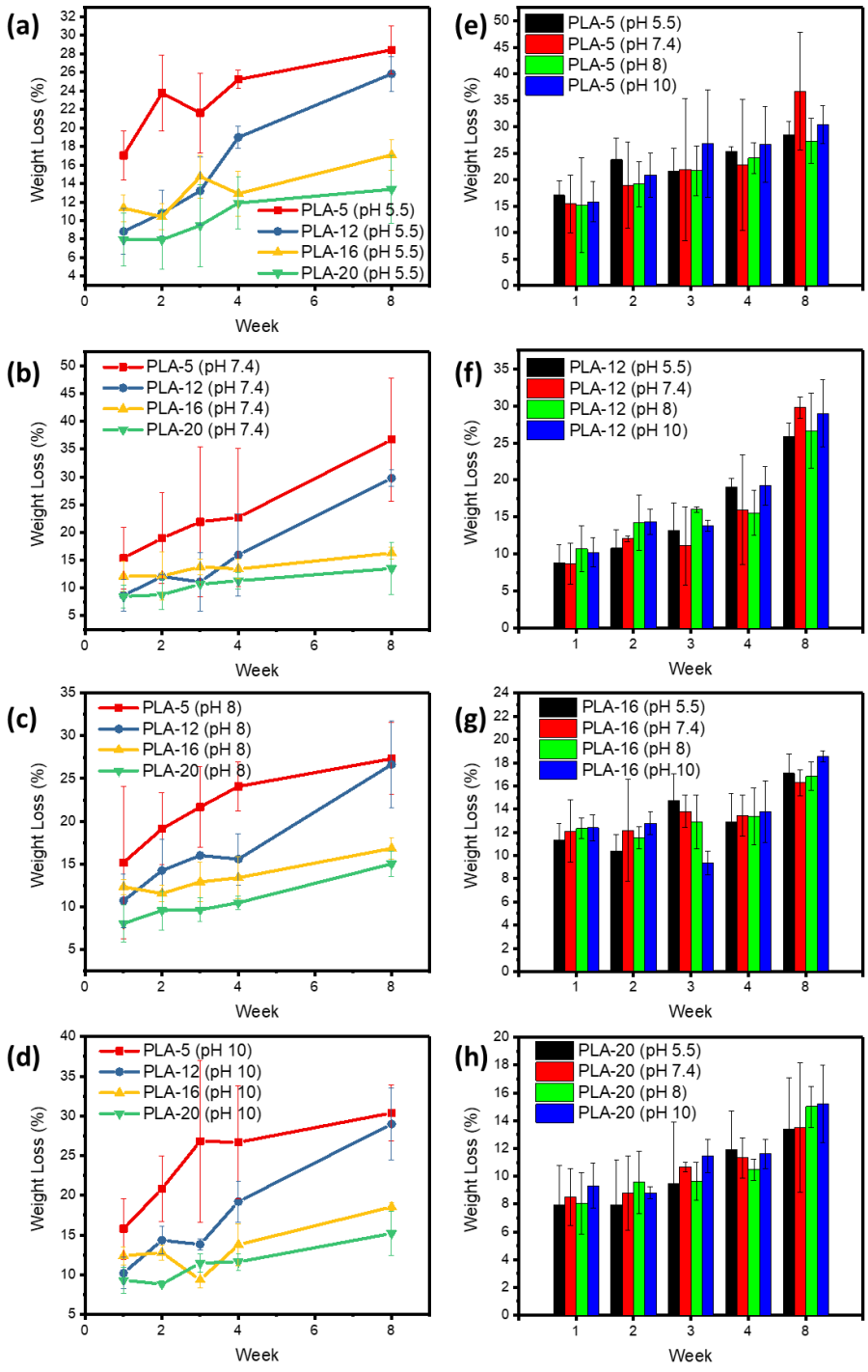

Figure 1. *Weight loss of PLA fiber with respect to duration of soaking (week), grouped according to (a) to (d): pH of soaking solution, (e) to (h): PLA fiber size.*

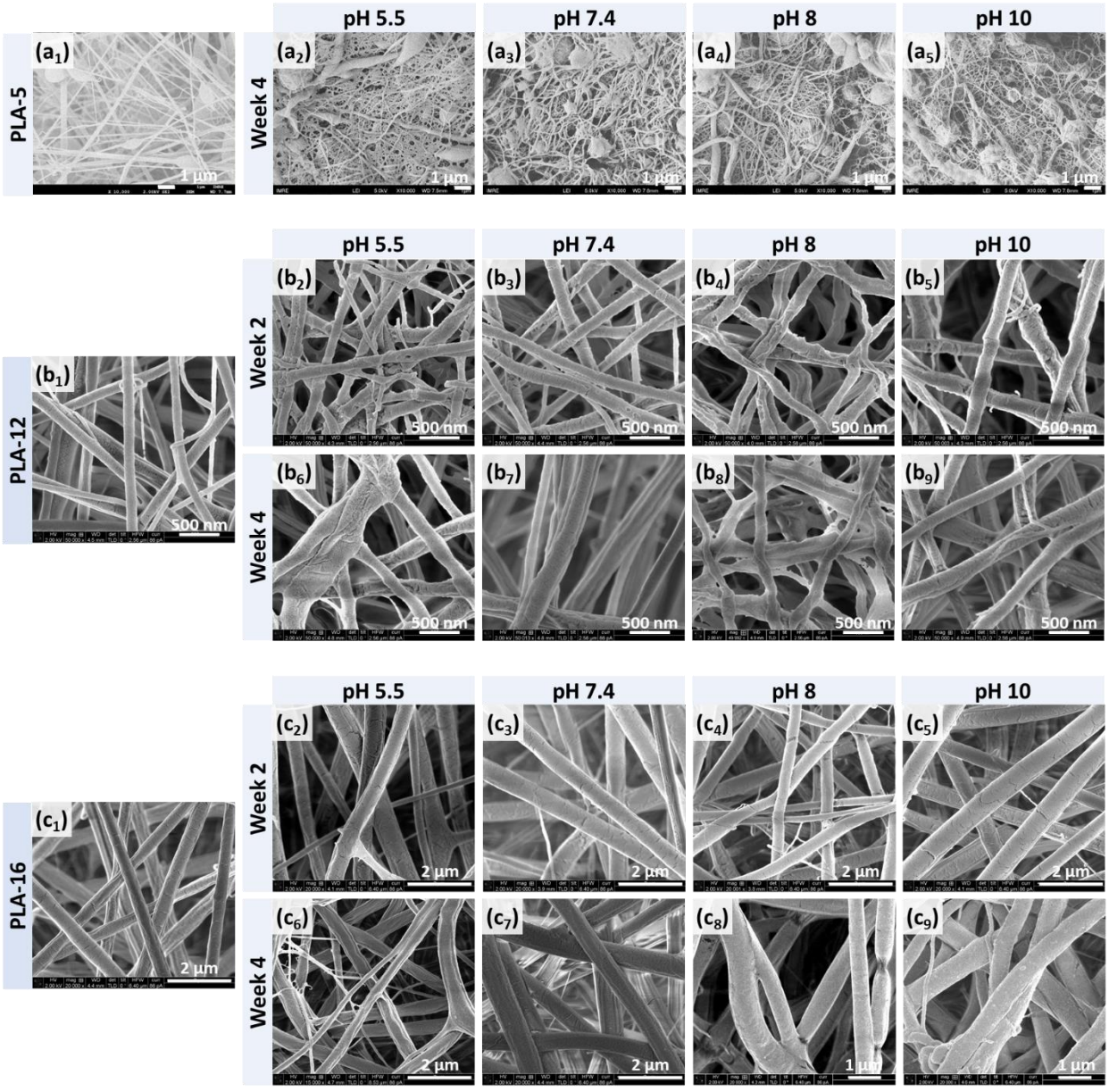

Figure 2. *SEM image of (a) PLA-5, (b) PLA-12, (c) PLA-16 after soaking in the respective pH environment for the designated duration.*

To study the effects of hydrolytic degradation under different pH environments on fiber morphology, surface analysis via SEM was conducted. PLA-5 fibers showed most severe

morphology deterioration especially at parts with less beading, after 4 weeks of soaking in the respective pH environment (Figure $2a_2 – a_5$). The SEM image of PLA-5 showed irregular shaped fibers and adhesion structures were seen throughout the fibrous mat. PLA-12 fibers soaked in pH 7.4 (Figure $2b_3$, b_7) showed minimal changes in surface morphology after 4 weeks with slight increase in adhesion structures between fiber strands (Figure $2b_1$). PLA-12 fibers soaked in both acid and base solutions started to show obvious degradation with irregular fibers and adhesion structures after week 2 (Figure $2b_2$, b_4, b_5). Fibers soaked in pH 8 and 10 appeared more eroded, indicating a faster degradation for PLA in alkaline conditions. The degradation features deteriorated in week 4 (Figure $2b_6$, b_8, b_9), which was comparatively worse for the fiber soaked in pH 5.5. As for PLA-16, due to the thicker fibers, no significant deterioration was observed for all fibers after soaking in the respective pH solution for 2 weeks (Figure $2c_2$ - c_5). After 4 weeks of soaking, fibers under pH 8 and pH 10 (Figure $2c_8$ and c_9) incurred minor adhesion structures, but overall maintaining the regular shape of the fiber strand. While the other fibers (Figure $2c_6$ and c_7) appeared to have no significant change in morphology. Given the minimal degradation in PLA-16, SEM analysis of PLA-20 was not carried out. This is in line with the $W_{\%L}$ trend, where PLA fibers with smaller diameter incurred greater degradation and $W_{\%L}$.

FTIR was performed to investigate the structural changes that took place during the hydrolytic degradation under various pH environment, where peak heights of the respective characteristic bands were compared. In order to eliminate any experimental influence, absorption peak height of the C=O and C-O bands were normalized against the CH_3 band, which is commonly used as an internal standard for PLA due to its inert nature.(Cuadri and Martín-Alfonso, 2018; Oliveira et al., 2016; Soo et al., 2022b) When comparing across the different sized PLA fibers soaked in different

310 pH environment (Figure 3a), there was slight deviation across the sample data which could be due
311 to inhomogeneity of the samples. However, in general there was no significant change in the C=O
312 or C-O peak ratios. A more in-depth analysis was conducted for PLA-12 (Figure 3b) since a
313 significant degradation was observed based on $W_{\%L}$ and morphology deterioration. However, no
314 significant change was detected even for samples soaked up to 8 weeks, which suggests that
315 degradation of the fibers occurred mainly via hydrolysis, where no additional C=O or C-O bonds
316 are formed. However, there was no detectable change in the intensity of the O-H band for degraded
317 fibers such as PLA-12 (pH 10) Wk 8 (Figure S2b), which further suggests that hydrolysis was not
318 widespread to generate a large amount of new -OH sites, but instead removed oligomer fragments
319 from the fibers to cause a significant $W_{\%L}$.
320

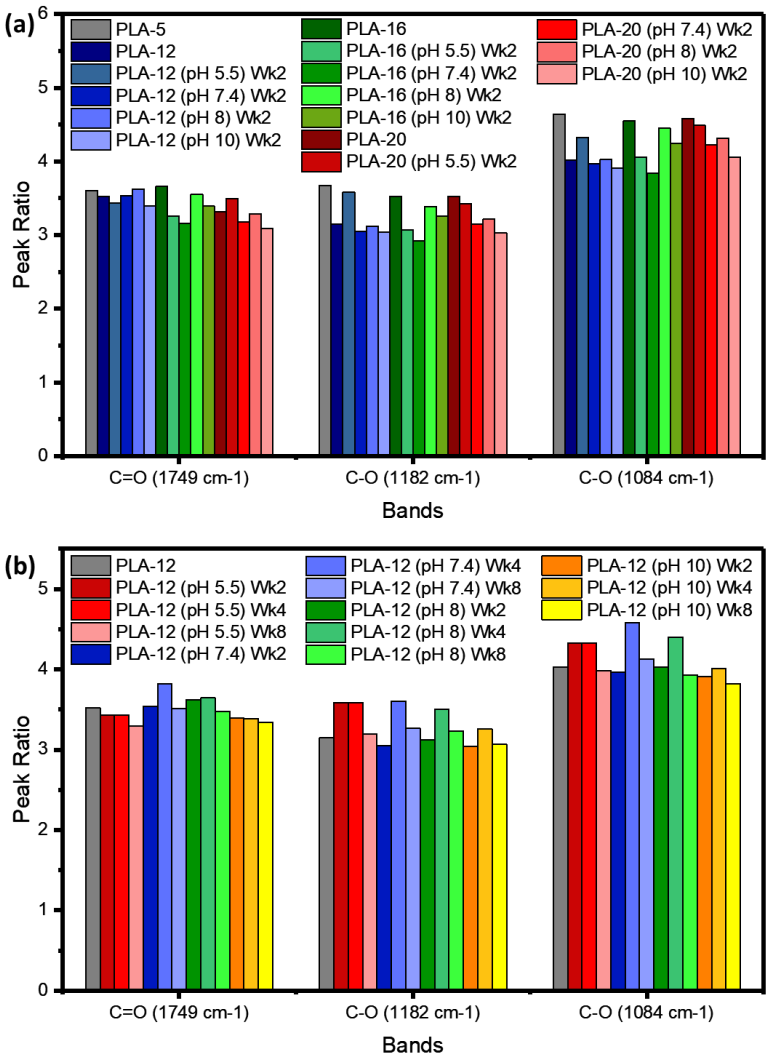

Figure 3. *Peak absorbance ratio of the C=O band at 1749cm^{-1}, and C-O bands at 1182 and 1084 cm^{-1} for (a) the original PLA-12, PLA-16 and PLA-20 fibers and their corresponding fibers soaked in different pH solution after 2 weeks, (b) original PLA-12 fiber and their corresponding fibers soaked in different pH solution after 2, 4 and 8 weeks.*

3.3 Biodegradation

In view of similar fiber diameter of PLA-12 and PLA-16, and similar degradation trends of PLA-16 and PLA-20, PLA-16 has been omitted for biodegradation studies. The averaged time-dependent biodegradation curves and first-order decay fitting results of the PLA fibers and references are shown in Figure 4 and Table S3. Biodegradation was initiated for all the samples after about one week of microbial lag and adaptation phase in inoculation.(Napper and Thompson, 2019; Pattanasuttichonlakul et al., 2018) By the end of 90 days, the biodegradation of cellulose paper plateaued at 79.1%, while the PLA fibers were at 10.0–22.8% and still slightly increasing. Therefore, the relative biodegradation degrees of the PLA compared to the cellulose were 12.2-27.9%. At the end of the test, the average weight loss (Table 1) of the PLA-5 (33.6%) was higher than that of the PLA-12 (16.8%) and PLA-20 (10.7%), which is consistent with the biodegradation trend shown in Figure 4. This trend is similar to hydrolytic degradation, where PLA with smaller diameter degraded at a faster rate. In view that SEM images of biodegraded fibers (Figure 5a) transited from smooth and regular fibers to rough and deformed with little or no pores, it suggests that biodegradation worked the same way as hydrolytic degradation, leading to surface erosion with minimal penetration to the bulk PLA.

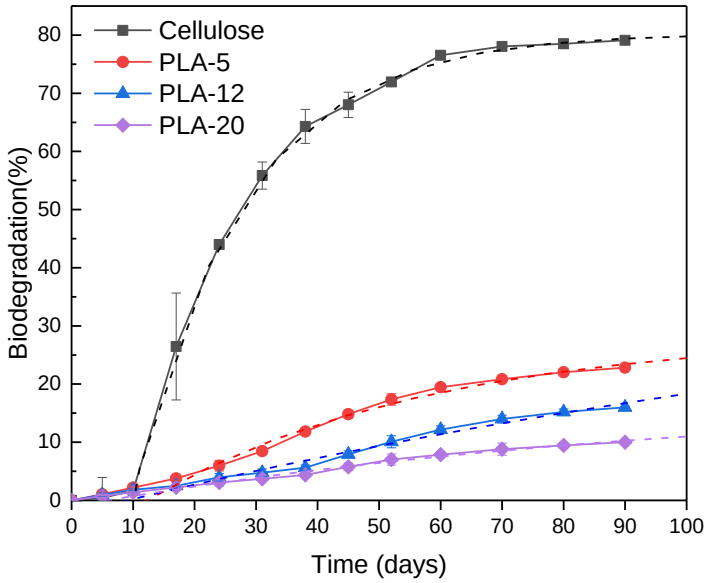

Figure 4. *Averaged time-dependent biodegradation of the PLA fibers and reference cellulose and the corresponding first-order decay fitting results.*

Table 1. *Weight loss of PLA fibers after biodegradation tests.*

	Initial weight (mg)	Final weight (mg)	Weight loss (mg)	Weight loss (%)	Average weight loss (%)
	98.3	65.4	32.9	33.5	
PLA-5	98.6	68.1	30.5	30.9	33.6
	97.4	62.0	35.4	36.3	
	96.9	83.4	13.5	13.9	
PLA-12	98	81.2	16.8	17.1	16.8
	99.3	80.0	19.3	19.4	
	97.4	89.0	8.4	8.6	
PLA-20	97.8	84.7	13.1	13.4	10.7
	98.3	88.3	10.0	10.2	

The morphology of the biodegraded fibers was analysed by SEM (Figure 5a) to visualize the effects of biodegradation. The biodegraded PLA-20 fibers remained regularly shaped with minor adhesion structures, which was consistent with the hydrolytic studies and low $W_{\%L}$. Biodegraded PLA-5 and PLA-12 fibers on the other hand displayed obvious irregularly shaped fibers and widespread adhesion structures, which was similar to the fibers subjected to hydrolytic degradation.

The FTIR analysis was carried out to analyze the structural change for biodegraded PLA fibers (Figure 5b). New absorption peaks corresponding to O-H stretch (3100-3600 cm^{-1}) and OH flexion (1631 cm^{-1}) bonds(del Rosario Salazar-Sánchez et al., 2019) were observed. When comparing the absorption peak height of the C=O and C-O bands that were normalized against the CH_3 band, the C-O band was found to significantly decrease for all samples, while changes in the C=O bonds was less significant (Figure 5c). Hydrolysis of PLA by the microorganisms resulted in an increase in the number of hydroxyl groups, which was detected as new O-H peaks in the FTIR analysis (Figure 5b). This suggests that a large number of PLA ester bond hydrolysis took place but does not lead to widespread cleavage of PLA oligomers from the bulk fibers. Instead, the large number of hydrolyzed segments remained on the PLA fiber, leading to a detectable increase in hydroxyl concentration by FTIR. In contrast to hydrolytic degradation where no O-H peak was detected in the degraded fibers, a large portion of hydrolyzed fragments possibly detached from main PLA fiber, which consequently led to a higher $W_{\%L}$ attained for PLA-12 and PLA-20 compared to biodegraded fibers. PLA-5 and PLA-20 have a lower intensity O-H peak than PLA-12. This may be due to formation of beads along the PLA-5 fibers that were five to eight times as large as the average fiber diameter (0.15 μm) and covered over 20 – 30% of the fibers' surface, which reduced the PLA-5 fiber's overall effective surface area exposed to biodegradation to similar to PLA-20.

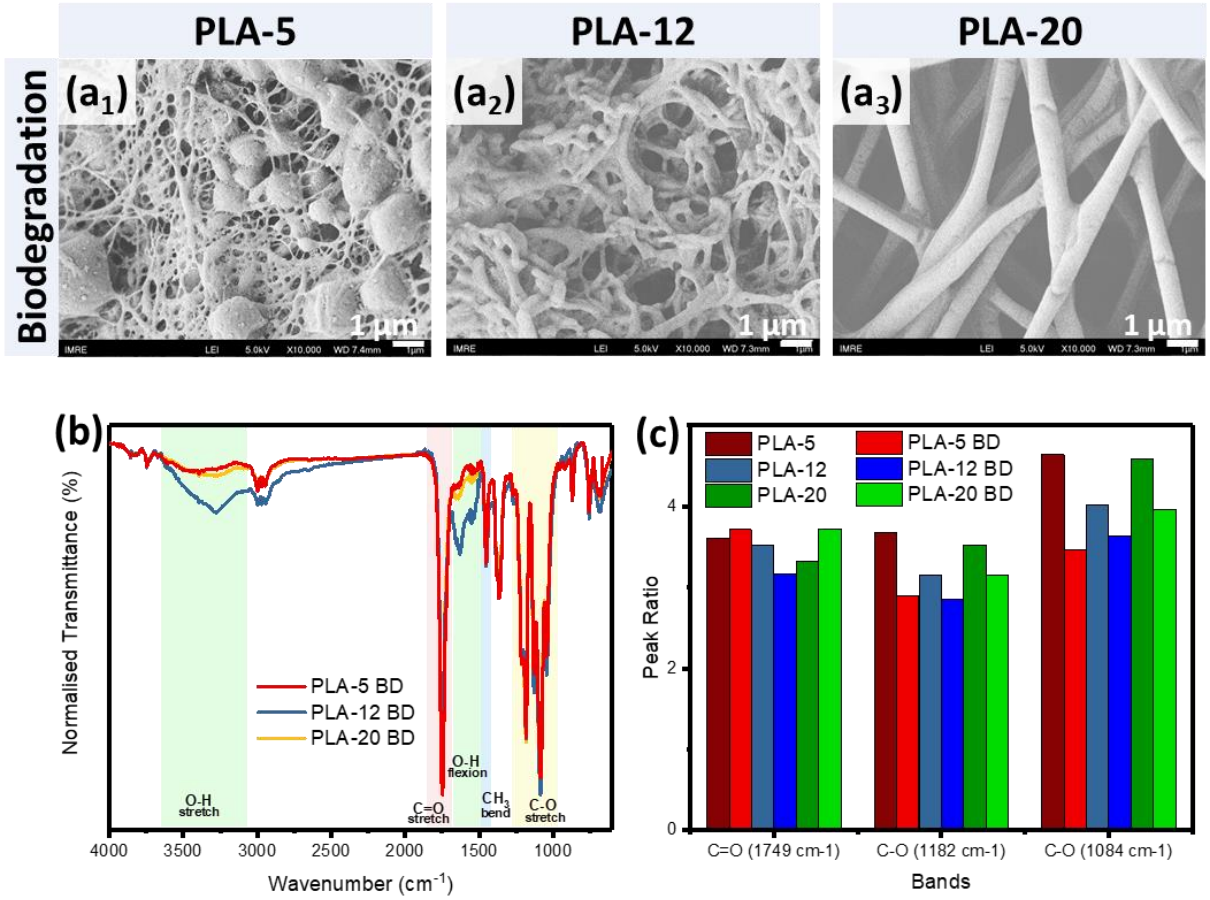

Figure 5. *(a) SEM analysis of PLA-5, 12 and 20 after biodegradation test. (b) FTIR analysis of PLA-5, PLA-12, PLA-20 after biodegradation studies. (c) Comparison of peak absorbance ratio of the C=O band at 1749cm^{-1}, and C-O bands at 1182 and 1084 cm^{-1} for original and biodegraded PLA fibers.*

3.4 Evaluation of fiber degradation performance

PLA displayed the ability to undergo hydrolytic and biodegradation, where in this study, the smallest fiber diameter, PLA-5, gave the best results of 30.71% and 33.60% $W_{\%L}$ respectively. However, excessive beading plagues the morphology of PLA-5, due to the limitation of the

fabrication process. This is not ideal for application, as poor uniformity in the fibers will weaken the structure, reduce surface area, and alter functional and mechanical properties. PLA-12 therefore appears the most promising with good morphology, and its hydrolytic degradation performance was only slightly lower than PLA-5 by 9%. Biodegradation effectiveness was slightly poorer compared to PLA-5 at 50% in terms of $W_{\%L}$, and 70% in terms of degree of biodegradation.

Nevertheless, the overall degradation rates are still rather low. In hydrolytic degradation, $W_{\%L}$ appears to rise rapidly in the first week, but with gradual increase thereafter. While for biodegradation, it appears to taper off after 60 days of exposure. This could be due to the constraints of the experimental design, where samples for both tests are soaked in the same degradation media throughout the test period. Therefore, initial pH and microorganism levels respectively are not sustained throughout to give a constant degradation activity. However, in natural environments, there may be continuous replacement of degradation media to maintain the level of degradation activity, and lead to higher levels of degradation with time.

In addition, PLA is a known biodegradable plastic, and has shown good biodegradability in compost and landfill conditions (up to 100% and 95%, respectively). However its biodegradation in marine environments is significantly slower (Van Roijen and Miller, 2022). The low biodegradation rate might be due to the absence of microorganisms that are efficient at PLA biodegradation in seawater media (Hino et al., 2023). Another contributing factor would be the lack of thermal energy for depolymerization of PLA in the marine environments (Chamas et al., 2020). Notably, the reduction of biodegradation rates in lab-scale tests is mainly related to the microorganisms, and the variations in its activity emphasize the influence of diverse environmental

407 factors, such as water temperature, nutrient depletion, and microbial competition. Our results are
408 in line with literature in highlighting the complex nature of PLA degradation in marine
409 environments. Further investigation on microbial communities and composition of intermediates
410 during the degradation process is needed for contributing to the broader discourse on the ecological
411 implications of PLA-based materials in marine ecosystems.
412

413 **4. Conclusion**

414 PLA fibers of different diameters were electrospun and found to be susceptible to both hydrolytic
415 degradation and biodegradation. In hydrolytic degradation, two-way ANOVA with replications
416 indicated a significant influence of varying the PLA diameter on $W_{\%L}$, where PLA fibers with small
417 diameter resulted in a faster degradation. Average $W_{\%L}$ was greatest for PLA-5 > PLA-12 > PLA-
418 16 > PLA-20 at 30.7%, 27.8%, 17.2% and 14.3% respectively. On the other hand, variations in pH
419 environment was found to have no significant influence on degradation rates, with $W_{\%L}$ almost
420 similar across each group. Biodegradation of PLA fibers showed similar trends of faster
421 degradation for fibers with small diameter, with PLA-5 giving the highest degree of biodegradation
422 at 22.8% followed by PLA-12 then PLA-20 at 16.0% and 10.0% respectively. Both degradation
423 methods led to more significant surface erosion and minimal bulk erosion, where SEM images
424 observed the transition of initial smooth and regular shaped fibers to rough and irregular shaped
425 fibers with little or no pores. The smaller diameter fibers incurred a deteriorated fiber morphology,
426 where PLA-5 and PLA-12 had increased adhesion structures and irregular fibers. While the fiber
427 morphology remained relatively unchanged for PLA-16 and PLA-20. In addition, new O-H peaks
428 were detected for biodegraded fibers but not hydrolytic degraded fibers, suggesting a higher
429 proportion of oligomer cleavage from PLA during hydrolytic degradation. Biodegradation in turn

gave rise to a larger number of hydrolyzed segments remaining on the PLA fiber, leading to a detectable increase in hydroxyl concentration by FTIR. Though our results are modest, it shows potential for more efficient PLA degradation via different methods by further engineering of the PLA morphology.

Future works can gear towards fabricating thinner and more uniform fibers by changing the molecular weight of the PLA polymer and therefore optimizing the solution concentration, viscosity, feed rate, voltage, drum rotation and needle movement speed etc. In addition, PLA can be electrospun with different polymer blends such starch, cellulose, polyhydroxyalkanoates, poly(butylene adipate-co-terephthalate) or other biodegradable polymers; or electrospun with appropriate catalysts or additives; or incorporate dissociative bonds in the PLA backbone to speed up the PLA degradation rate and percentage of material that is metabolized or solubilized. This would improve the degradability of PLA based fibers and open up new areas of application for this material.

Declaration of competing interest

The authors declare that they have no known competing financial interests or personal relationships that could have appeared to influence the work reported in this paper.

Acknowledgement

This work was supported under the Structural Metal Alloy Program (SMAP), Grant No. A18b1B0061, in Agency for Science, Technology and Research in Singapore.

References

Álvarez-Chávez, C.R., Edwards, S., Moure-Eraso, R., Geiser, K., 2012. Sustainability of bio-based plastics: general comparative analysis and recommendations for improvement. J. Clean. Prod. 23 (1), 47-56. https://doi.org/10.1016/j.jclepro.2011.10.003.

Amorin, N.S., Rosa, G., Alves, J.F., Gonçalves, S.P., Franchetti, S.M., Fechine, G.J., 2014. Study of thermodegradation and thermostabilization of poly (lactide acid) using subsequent extrusion cycles. J. Appl. Polym. Sci. 131 (6). https://doi.org/10.1002/app.40023.

Araque-Monrós, M.C., Vidaurre, A., Gil-Santos, L., Gironés Bernabé, S., Monleón-Pradas, M., Más-Estellés, J., 2013. Study of the degradation of a new PLA braided biomaterial in buffer phosphate saline, basic and acid media, intended for the regeneration of tendons and ligaments. Polym. Degrad. Stab. 98 (9), 1563-1570. https://doi.org/10.1016/j.polymdegradstab.2013.06.031.

Atiwesh, G., Mikhael, A., Parrish, C.C., Banoub, J., Le, T.-A.T., 2021. Environmental impact of bioplastic use: A review. Heliyon 7 (9), e07918. https://doi.org/10.1016/j.heliyon.2021.e07918.

Benson, N.U., Fred-Ahmadu, O.H., Bassey, D.E., Atayero, A.A., 2021. COVID-19 pandemic and emerging plastic-based personal protective equipment waste pollution and management in Africa. Journal of Environmental Chemical Engineering 9 (3), 105222. https://doi.org/10.1016/j.jece.2021.105222.

Brodin, M., Vallejos, M., Opedal, M.T., Area, M.C., Chinga-Carrasco, G., 2017. Lignocellulosics as sustainable resources for production of bioplastics – A review. J. Clean. Prod. 162, 646-664. https://doi.org/10.1016/j.jclepro.2017.05.209.

475 Campanaro, A.L., Simcik, M.F., Maurer-Jones, M.A., Penn, R.L., 2023. Sewage sludge induces
476 changes in the surface chemistry and crystallinity of polylactic acid and polyethylene
477 films. Sci. Total Environ. 890, 164313. https://doi.org/10.1016/j.scitotenv.2023.164313.
478 Chamas, A., Moon, H., Zheng, J., Qiu, Y., Tabassum, T., Jang, J.H., Abu-Omar, M., Scott, S.L.,
479 Suh, S., 2020. Degradation Rates of Plastics in the Environment. ACS Sustainable
480 Chemistry & Engineering 8 (9), 3494-3511. 10.1021/acssuschemeng.9b06635.
481 Choi, S., Jeon, H., Jang, M., Kim, H., Shin, G., Koo, J.M., Lee, M., Sung, H.K., Eom, Y., Yang,
482 H.S., 2021. Biodegradable, efficient, and breathable multi-use face mask filter. Adv. Sci.
483 8 (6), 2003155. https://doi.org/10.1002/advs.202003155.
484 Cuadri, A.A., Martín-Alfonso, J.E., 2018. Thermal, thermo-oxidative and thermomechanical
485 degradation of PLA: A comparative study based on rheological, chemical and thermal
486 properties. Polym. Degrad. Stab. 150, 37-45.
487 https://doi.org/10.1016/j.polymdegradstab.2018.02.011.
488 Cui, G., Bai, Y., Li, W., Gao, Z., Chen, S., Qiu, N., Satoh, T., Kakuchi, T., Duan, Q., 2017.
489 Synthesis and characterization of Eu(III) complexes of modified d-glucosamine and
490 poly(N-isopropylacrylamide). Materials Science and Engineering: C 78, 603-608.
491 https://doi.org/10.1016/j.msec.2017.03.059.
492 Cui, G., Zhao, K., You, K., Gao, Z., Kakuchi, T., Feng, B., Duan, Q., 2020. Synthesis and
493 characterization of phenylboronic acid-containing polymer for glucose-triggered drug
494 delivery+. Science and Technology of Advanced Materials 21 (1), 1-10.
495 https://doi.org/10.1080/14686996.2019.1700394.
496 del Rosario Salazar-Sánchez, M., Campo-Erazo, S.D., Villada-Castillo, H.S., Solanilla-Duque,
497 J.F., 2019. Structural changes of cassava starch and polylactic acid films submitted to

biodegradation process. International Journal of Biological Macromolecules 129, 442-447. https://doi.org/10.1016/j.ijbiomac.2019.01.187.

Dharmaraj, S., Ashokkumar, V., Hariharan, S., Manibharathi, A., Show, P.L., Chong, C.T., Ngamcharussrivichai, C., 2021. The COVID-19 pandemic face mask waste: A blooming threat to the marine environment. Chemosphere 272, 129601. https://doi.org/10.1016/j.chemosphere.2021.129601.

Dong, S., Zhang, H., Yuan, D., 2023. Supramolecular Nonwoven Materials via Thermally Induced Precursor Crystallization of Nanocrystalline Fibers/Belts for Recyclable Air Filters. ACS Appl. Nano Mater. 6 (11), 9548-9557. 10.1021/acsanm.3c01254.

Dunne, M., Corrigan, O.I., Ramtoola, Z., 2000. Influence of particle size and dissolution conditions on the degradation properties of polylactide-co-glycolide particles. Biomater. 21 (16), 1659-1668. https://doi.org/10.1016/S0142-9612(00)00040-5.

El-malek, F.A., Khairy, H., Farag, A., Omar, S., 2020. The sustainability of microbial bioplastics, production and applications. International Journal of Biological Macromolecules 157, 319-328. https://doi.org/10.1016/j.ijbiomac.2020.04.076.

Fan, X., Tan, B.H., Li, Z., Loh, X.J., 2017. Control of PLA stereoisomers-based polyurethane elastomers as highly efficient shape memory materials. ACS Sustain. Chem. Eng. 5 (1), 1217-1227. https://doi.org/10.1021/acssuschemeng.6b02652.

Garcia, R.A., Stevanovic, T., Berthier, J., Njamen, G., Tolnai, B., Achim, A., 2021. Cellulose, Nanocellulose, and Antimicrobial Materials for the Manufacture of Disposable Face Masks: A Review. BioResources 16 (2).

519 Grizzi, I., Garreau, H., Li, S., Vert, M., 1995. Hydrolytic degradation of devices based on
520 poly(dl-lactic acid) size-dependence. Biomater. 16 (4), 305-311.
521 https://doi.org/10.1016/0142-9612(95)93258-F.
522 Guo, Z., Zhan, R., Shi, Y., Zhu, D., Pan, J., Yang, C., Wang, Y., Wang, J., 2023. Innovative and
523 green utilization of zinc-bearing dust by hydrogen reduction: Recovery of zinc and lead,
524 and synergetic preparation of Fe/C micro-electrolysis materials. Chem. Eng. J. 456,
525 141157. https://doi.org/10.1016/j.cej.2022.141157.
526 He, H., Gao, M., Illés, B., Molnar, K., 2020. 3D printed and electrospun, transparent, hierarchical
527 polylactic acid mask nanoporous filter. International journal of bioprinting 6 (4).
528 https://doi.org/10.18063/ijb.v6i4.278.
529 Hino, S., Kawasaki, N., Yamano, N., Nakamura, T., Nakayama, A., 2023. Effects of particle size
530 on marine biodegradation of poly(l-lactic acid) and poly(ε-caprolactone). Materials
531 Chemistry and Physics 303. 10.1016/j.matchemphys.2023.127813.
532 Iñiguez-Franco, F., Auras, R., Rubino, M., Dolan, K., Soto-Valdez, H., Selke, S., 2017. Effect of
533 nanoparticles on the hydrolytic degradation of PLA-nanocomposites by water-ethanol
534 solutions. Polym. Degrad. Stab. 146, 287-297.
535 https://doi.org/10.1016/j.polymdegradstab.2017.11.004.
536 ISO, 2020. ISO 19679: 2020 Plastics — Determination of aerobic biodegradation of non-floating
537 plastic materials in a seawater/sediment interface — Method by analysis of evolved
538 carbon dioxide. https://www.iso.org/standard/78889.html.
539 Kalendova, A., Smotek, J., Stloukal, P., Kracalik, M., Slouf, M., Laske, S., 2019. Transport
540 properties of poly (lactic acid)/clay nanocomposites. Polymer Engineering & Science 59
541 (12), 2498-2501. https://doi.org/10.1002/pen.25251.

542 Lagaron, J.M., Lopez-Rubio, A., 2011. Nanotechnology for bioplastics: opportunities, challenges
543 and strategies. Trends in Food Science & Technology 22 (11), 611-617.
544 https://doi.org/10.1016/j.tifs.2011.01.007.
545 Lee, J.J.C., Sugiarto, S., Ong, P.J., Soo, X.Y.D., Ni, X., Luo, P., Hnin, Y.Y.K., See, J.S.Y., Wei, F.,
546 Zheng, R., 2022. Lignin-g-polycaprolactone as a form-stable phase change material for
547 thermal energy storage application. J. Energy Storage 56, 106118.
548 https://doi.org/10.1016/j.est.2022.106118.
549 Liang, R., Yang, X., Yew, P.Y.M., Sugiarto, S., Zhu, Q., Zhao, J., Loh, X.J., Zheng, L., Kai, D.,
550 2022. PLA-lignin nanofibers as antioxidant biomaterials for cartilage regeneration and
551 osteoarthritis treatment. Journal of Nanobiotechnology 20 (1), 327.
552 https://doi.org/10.1186/s12951-022-01534-2.
553 Lim, Q.F., Yap, R.C.C., Teng, C.P., Yeo, J.C.C., Tan, M.Y., Toh, J.P.W., Zhu, Q., Thitsartarn, W.,
554 He, C., Liu, S., 2023. Electrospray-on-Electrospun Breathable, Biodegradable, and
555 Robust Nanofibrous Membranes with Photocatalytic Bactericidal Activity. ACS Appl.
556 Nano Mater. 6 (3), 1828-1838. https://doi.org/10.1021/acsanm.2c04776.
557 Limsukon, W., Auras, R., Selke, S., 2019. Hydrolytic degradation and lifetime prediction of
558 poly(lactic acid) modified with a multifunctional epoxy-based chain extender. Polym.
559 Test. 80, 106108. https://doi.org/10.1016/j.polymertesting.2019.106108.
560 Loh, X.J., 2013. Poly (DMAEMA-co-PPGMA): Dual-responsive “reversible” micelles. J. Appl.
561 Polym. Sci. 127 (2), 992-1000. https://doi.org/10.1002/app.37530.
562 Luo, Y.-B., Wang, X.-L., Wang, Y.-Z., 2012. Effect of TiO2 nanoparticles on the long-term
563 hydrolytic degradation behavior of PLA. Polym. Degrad. Stab. 97 (5), 721-728.
564 https://doi.org/10.1016/j.polymdegradstab.2012.02.011.

565 Madhavan Nampoothiri, K., Nair, N.R., John, R.P., 2010. An overview of the recent
566 developments in polylactide (PLA) research. Bioresour. Technol. 101 (22), 8493-8501.
567 https://doi.org/10.1016/j.biortech.2010.05.092.
568 Mitchell, M.K., Hirt, D.E., 2015. Degradation of PLA fibers at elevated temperature and
569 humidity. Polymer Engineering & Science 55 (7), 1652-1660.
570 https://doi.org/10.1002/pen.24003.
571 Morganti, P., Morganti, G., 2020. Post-COVID-19: An Opportunity to Produce Biodegradable
572 Goods & Surgical Masks to Save the Environment. Journal of Health Care and Research
573 1 (3), 157. https://doi.org/10.36502/2020/hcr.6174.
574 Morganti, P., Yudin, V.E., Morganti, G., Coltelli, M.-B., 2020. Trends in surgical and beauty
575 masks for a cleaner environment. Cosmetics 7 (3), 68.
576 https://doi.org/10.3390/cosmetics7030068.
577 Muiruri, J.K., Yeo, J.C.C., Soo, X.Y.D., Wang, S., Liu, H., Kong, J., Cao, J., Tan, B.H., Suwardi,
578 A., Li, Z., 2023. Recent Advances of Sustainable Short-chain length
579 Polyhydroxyalkanoates (Scl-PHAs)–Plant Biomass Composites. Eur. Polym. J., 111882.
580 https://doi.org/10.1016/j.eurpolymj.2023.111882.
581 Muiruri, J.K., Yeo, J.C.C., Zhu, Q., Ye, E., Loh, X.J., Li, Z., 2022. Poly (hydroxyalkanoates):
582 Production, applications and end-of-life strategies–life cycle assessment nexus. ACS
583 Sustain. Chem. Eng. 10 (11), 3387-3406.
584 https://doi.org/10.1021/acssuschemeng.1c08631.
585 Napper, I.E., Thompson, R.C., 2019. Environmental Deterioration of Biodegradable, Oxo-
586 biodegradable, Compostable, and Conventional Plastic Carrier Bags in the Sea, Soil, and

Open-Air Over a 3-Year Period. Environ. Sci. Technol. 53 (9), 4775-4783. https://doi.org/10.1021/acs.est.8b06984.

Nguyen, V.P.N., Kuo, N., Loh, X.J., 2011. New biocompatible thermogelling copolymers containing ethylene-butylene segments exhibiting very low gelation concentrations. Soft Matter 7 (5), 2150-2159. https://doi.org/10.1039/C0SM00764A.

OECD, 1992a. OECD 301: Guideline for Testing of Chemicals - Ready Biodegradability. https://www.oecd.org/chemicalsafety/risk-assessment/1948209.pdf (Accessed on 14 Feb 2023).

OECD, 1992b. OECD 306: Guideline for Testing of Chemicals - Biodegradability in Seawater. https://www.oecd-ilibrary.org/docserver/9789264070486-en.pdf?expires=1676358553&id=id&accname=guest&checksum=180531B27975EAE31421D2FC67E2C6AC (Accessed on 14 Feb 2023).

Oliveira, M., Santos, E., Araújo, A., Fechine, G.J.M., Machado, A.V., Botelho, G., 2016. The role of shear and stabilizer on PLA degradation. Polym. Test. 51, 109-116. https://doi.org/10.1016/j.polymertesting.2016.03.005.

Ozdemir, E., Lekesiz, T.O., Hacaloglu, J., 2016. Polylactide/organically modified montmorillonite composites; effects of organic modifier on thermal characteristics. Polym. Degrad. Stab. 134, 87-96. https://doi.org/10.1016/j.polymdegradstab.2016.09.028.

Pang, S., Zhou, C., Sun, Y., Zhang, K., Ye, W., Zhao, X., Cai, L., Hui, B., 2023. Natural wood-derived charcoal embedded with bimetallic iron/cobalt sites to promote ciprofloxacin degradation. J. Clean. Prod. 414, 137569. https://doi.org/10.1016/j.jclepro.2023.137569.

609 Patil, N.A., Gore, P.M., Jaya Prakash, N., Govindaraj, P., Yadav, R., Verma, V., Shanmugarajan,
610 D., Patil, S., Kore, A., Kandasubramanian, B., 2021. Needleless electrospun
611 phytochemicals encapsulated nanofibre based 3-ply biodegradable mask for combating
612 COVID-19 pandemic. Chem. Eng. J. 416, 129152.
613 https://doi.org/10.1016/j.cej.2021.129152.
614 Pattanasuttichonlakul, W., Sombatsompop, N., Prapagdee, B., 2018. Accelerating biodegradation
615 of PLA using microbial consortium from dairy wastewater sludge combined with PLA-
616 degrading bacterium. International Biodeterioration & Biodegradation 132, 74-83.
617 https://doi.org/10.1016/j.ibiod.2018.05.014.
618 Png, Z.M., Wang, C.-G., Yeo, J., Lee, J.J.C., Surat'man, N.E.B., Tan, Y.L., Liu, H., Wang, P., Tan,
619 M.B.H., Xu, J., 2023. Stimuli-responsive Structure-Property Switchable Polymer
620 Materials. Mol. Syst. Des. Eng. https://doi.org/10.1039/D3ME00002H.
621 Richert, A., Dąbrowska, G.B., 2021. Enzymatic degradation and biofilm formation during
622 biodegradation of polylactide and polycaprolactone polymers in various environments.
623 International Journal of Biological Macromolecules 176, 226-232.
624 https://doi.org/10.1016/j.ijbiomac.2021.01.202.
625 Santoro, M., Shah, S.R., Walker, J.L., Mikos, A.G., 2016. Poly(lactic acid) nanofibrous scaffolds
626 for tissue engineering. Advanced Drug Delivery Reviews 107, 206-212.
627 https://doi.org/10.1016/j.addr.2016.04.019.
628 Sarasa, J., Gracia, J.M., Javierre, C., 2009. Study of the biodisintegration of a bioplastic material
629 waste. Bioresour. Technol. 100 (15), 3764-3768.
630 https://doi.org/10.1016/j.biortech.2008.11.049.

631 Soo, X.Y., Muiruri, J.K., Yeo, J.C., Png, Z.M., Sng, A., Xie, H., Ji, R., Wang, S., Liu, H., Xu, J.,
632 2023. Polyethylene glycol/polylactic acid block co-polymers as solid–solid phase change
633 materials. SmartMat, e1188. https://doi.org/10.1002/smm2.1188.
634 Soo, X.Y.D., Png, Z.M., Wang, X., Chua, M.H., Ong, P.J., Wang, S., Li, Z., Chi, D., Xu, J., Loh,
635 X.J., Zhu, Q., 2022a. Rapid UV-curable form-stable polyethylene-glycol-based phase
636 change material. ACS Appl. Polym. Mater. 4 (4), 2747-2756.
637 https://doi.org/10.1021/acsapm.2c00059.
638 Soo, X.Y.D., Wang, S., Yeo, C.C.J., Li, J., Ni, X.P., Jiang, L., Xue, K., Li, Z., Fei, X., Zhu, Q.,
639 Loh, X.J., 2022b. Polylactic acid face masks: Are these the sustainable solutions in times
640 of COVID-19 pandemic? Sci. Total Environ. 807, 151084.
641 https://doi.org/10.1016/j.scitotenv.2021.151084.
642 Surrao, D.C., Waldman, S.D., Amsden, B.G., 2012. Biomimetic poly(lactide) based fibrous
643 scaffolds for ligament tissue engineering. Acta Biomater. 8 (11), 3997-4006.
644 https://doi.org/10.1016/j.actbio.2012.07.012.
645 Tang, T., Zhou, M., Lv, J., Cheng, H., Wang, H., Qin, D., Hu, G., Liu, X., 2022. Sensitive and
646 selective electrochemical determination of uric acid in urine based on ultrasmall iron
647 oxide nanoparticles decorated urchin-like nitrogen-doped carbon. Colloids and Surfaces
648 B: Biointerfaces 216, 112538. https://doi.org/10.1016/j.colsurfb.2022.112538.
649 Vaid, R., Yildirim, E., Pasquinelli, M.A., King, M.W., 2021. Hydrolytic degradation of polylactic
650 acid fibers as a function of ph and exposure time. Molecules 26 (24), 7554.
651 https://doi.org/10.3390/molecules26247554.

652 Van Roijen, E.C., Miller, S.A., 2022. A review of bioplastics at end-of-life: Linking experimental
653 biodegradation studies and life cycle impact assessments. Resources, Conservation and
654 Recycling 181. 10.1016/j.resconrec.2022.106236.
655 Wang, L., Du, Y., Zhu, Q., Song, J., Ou, K., Xie, G., Yu, Z., 2023. Regulating the Alkyl Chain
656 Length of Quaternary Ammonium Salt to Enhance the Inkjet Printing Performance on
657 Cationic Cotton Fabric with Reactive Dye Ink. ACS Appl. Mater. Interfaces 15 (15),
658 19750-19760. 10.1021/acsami.3c02304.
659 Wang, L., Gao, Y., Xiong, J., Shao, W., Cui, C., Sun, N., Zhang, Y., Chang, S., Han, P., Liu, F.,
660 He, J., 2022a. Biodegradable and high-performance multiscale structured nanofiber
661 membrane as mask filter media via poly(lactic acid) electrospinning. J. Colloid Interface
662 Sci. 606, 961-970. https://doi.org/10.1016/j.jcis.2021.08.079.
663 Wang, S., Muiruri, J.K., Soo, X.Y.D., Liu, S., Thitsartarn, W., Tan, B.H., Suwardi, A., Li, Z.,
664 Zhu, Q., Loh, X.J., 2022b. Bio-Polypropylene and Polypropylene-based Biocomposites:
665 Solutions for a Sustainable Future. Chem. Asian J., e202200972.
666 https://doi.org/10.1002/asia.202200972
667 Wang, S., Ong, P.J., Liu, S., Thitsartarn, W., Tan, M.J.B.H., Suwardi, A., Zhu, Q., Loh, X.J.,
668 2022c. Recent Advances in Host-Guest Supramolecular Hydrogels for Biomedical
669 Applications. Chem. Asian J. 17 (18), e202200608.
670 https://doi.org/10.1002/asia.202200608.
671 Xu, L., Crawford, K., Gorman, C.B., 2011. Effects of temperature and pH on the degradation of
672 poly (lactic acid) brushes. Macromolecules 44 (12), 4777-4782.
673 https://doi.org/10.1021/ma2000948.

Yusoff, N.H., Pal, K., Narayanan, T., de Souza, F.G., 2021. Recent trends on bioplastics synthesis and characterizations: Polylactic acid (PLA) incorporated with tapioca starch for packaging applications. J. Mol. Struct. 1232, 129954. https://doi.org/10.1016/j.molstruc.2021.129954.

Zhang, L., Qin, D., Feng, J., Tang, T., Cheng, H., 2023. Rapid quantitative detection of luteolin using an electrochemical sensor based on electrospinning of carbon nanofibers doped with single-walled carbon nanoangles. Analytical Methods 15 (25), 3073-3083. https://doi.org/10.1039/D3AY00497J.

Zhao, Q., Wang, Y., Zhu, Z., Zhao, Q., Zhu, L., Jiang, L., 2023. Efficient reduction of β-lactoglobulin allergenicity in milk using Clostridium tyrobutyricum Z816. Food Science and Human Wellness 12 (3), 809-816. https://doi.org/10.1016/j.fshw.2022.09.017.

Zheng, Y., Liu, Y., Guo, X., Chen, Z., Zhang, W., Wang, Y., Tang, X., Zhang, Y., Zhao, Y., 2020. Sulfur-doped g-C3N4/rGO porous nanosheets for highly efficient photocatalytic degradation of refractory contaminants. Journal of Materials Science & Technology 41, 117-126. https://doi.org/10.1016/j.jmst.2019.09.018.